



TEM analysis and wear resistance of the ceramic coatings on Q235 steel prepared by hybrid method of hot-dipping aluminum and plasma electrolytic oxidation

Lu Lihong^{a,b}, Zhang Jingwu^a, Shen Dejiu^{a,*}, Wu Lailei^a, Jiang Guirong^a, Li Liang^c

^a State Key Laboratory of Metastable Materials Science and Technology, College of Materials Science and Engineering, Yanshan University, Qinhuangdao 066004, PR China

^b Science and Research Department, The Chinese People's Armed Police Academy, Langfang 065000, PR China

^c State Key Laboratory of Automotive Safety and Energy, Tsinghua University, Beijing 100084, PR China

ARTICLE INFO

Article history:

Received 18 April 2011

Received in revised form 28 August 2011

Accepted 30 August 2011

Available online 22 September 2011

Keywords:

Plasma electrolytic oxidation

Hot-dipping aluminum

TEM

Hardness

Wear resistance

ABSTRACT

The hybrid method of PEO and hot-dipping aluminum (HDA) was employed to deposit composite ceramic coatings on the surface of Q235 steel. The composition of the composite coatings was investigated with X-ray diffraction (XRD) and transmission electron microscopy (TEM), respectively. The cross-section microstructure and micro-hardness of the treated specimens were investigated and analyzed with scanning electron microscopy (SEM) and microscopic hardness meter (MHM), respectively. The wear resistance of the ceramic coatings was investigated by a self-made rubbing wear testing machine. The results indicate that metallurgical bonding can be observed between the ceramic coatings and the steel substrate. There are many micro-pores and micro-cracks, which act as the discharge channels and result of quick and non-uniform cooling of melted sections in the plasma electrolytic oxidation ceramic coatings. The phase composition of the ceramic coatings is mainly composed of amorphous phase and crystal Al_2O_3 oxides. The crystal Al_2O_3 phase includes $\kappa\text{-Al}_2\text{O}_3$, $\theta\text{-Al}_2\text{O}_3$ and $\beta\text{-Al}_2\text{O}_3$. The grain size of the $\kappa\text{-Al}_2\text{O}_3$ crystal is quite non-uniform. The hardness of the ceramic coatings is about HV1300 and 10 times higher than that of the Q235 substrate, which was favorable to the better wear resistance of the ceramic coatings.

© 2011 Elsevier B.V. All rights reserved.

1. Introduction

Plasma electrolytic oxidation (PEO), or micro-arc oxidation (MAO), is a novel electro-chemical surface treatment process for generating oxide coatings on valuable metals such as Al, Mg, Ti and their alloys [1–3]. It can be employed to produce thick (e.g. 50–150 μm), hard ceramic coatings, with improved thermo-mechanical, wear and corrosion resistance properties compared with conventional anodizing technique [4–8]. However, the technology is hard to be directly applied to steels, which are the most widely used materials in engineering structures, since steels do not have the same characters as the valve metals.

In order to employ the advanced surface modification technology for steel surface, researchers have tried to use indirect ways to get ceramic coatings on steels, Shen and Wu et al. got ceramic coatings by a hybrid method of hot-dipping aluminum on steels and micro-arc anodizing the hot-dipped aluminum [9,10]. Gu and Pokhmurskii et al. got ceramic coatings by method of micro-arc oxidation after arc spraying aluminum on steels [11,12]. Compared

with arc sprayed aluminum layer, hot-dipped aluminum layer has higher bonding strength to the steel substrates due to the metallurgical bonding between the aluminum layers and the steel substrate. So the hybrid method of micro-arc oxidation after hot dipping aluminizing (HDA) is very promising to be used to prepare this kind of protective composite ceramic coatings on steel surface.

In this paper, aluminum layer was firstly prepared by HDA on Q235 steel substrate, and then ceramic coatings was deposited on the aluminum layer using PEO. The phase composition, the microstructure, the wear resistance of the composite coatings and the cross-section micro-hardness of the treated samples were investigated. Particularly, transmission electron microscopy (TEM), which was used by Nie et al. to investigate the cross-sectional microstructure of the PEO coatings on a magnesium engine AJ62 alloy [13], was firstly used to analyze the phase composition of the ceramic coatings in this paper.

2. Experimental

Rectangular coupons (25 mm \times 10 mm \times 2.5 mm) made of Q235 steel (C 0.14–0.22%, Mn 0.30–0.65%, Si 0.3%, S 0.05%, P 0.045%, Fe balance) were used as the initial substrates. An industrial pure aluminum L1 (Cu 0.01%, Fe 0.16%, Fe+Si 0.26%, other impurities 0.03%, Al balance) was used as the hot-dipping material. The main parameters of the hot-dipping process, i.e. temperature and time, are 2 min at

* Corresponding author. Tel.: +86 335 8055799.

E-mail address: sdj217@ysu.edu.cn (D. Shen).

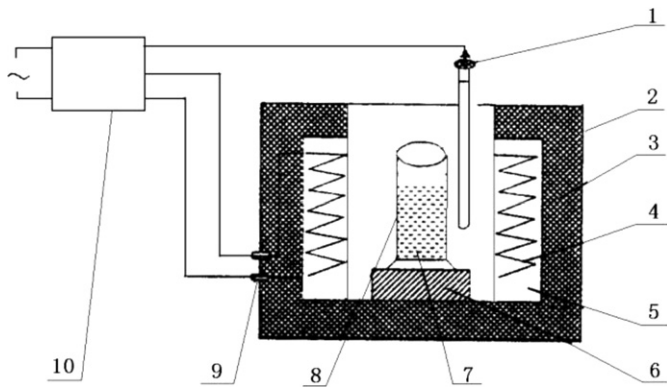


Fig. 1. Schematic drawing of the aluminum hot-dipping equipment. 1 – Thermocouple; 2 – furnace shell; 3 – asbestos insert; 4 – resistance wire; 5 – gray porcelain tube; 6 – firebrick; 7 – molten aluminum; 8 – aluminum melting pot; 9 – quartz tube; 10 – temperature controller for resistance furnace.

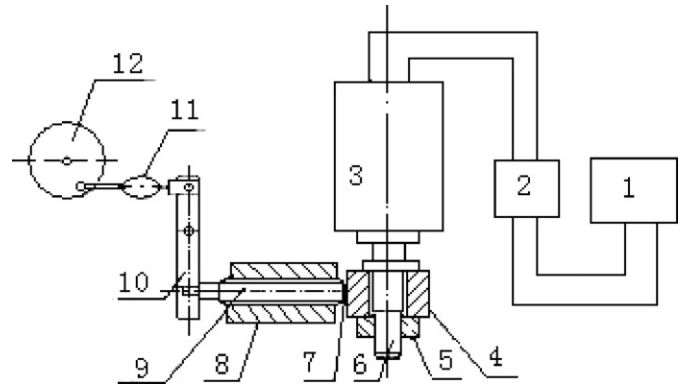


Fig. 3. The schematic of the equipment for the wearing experiment. 1 – electrical source; 2 – autotransformer; 3 – engine; 4 – cast iron; 5 – clamp nut; 6 – output axis; 7 – sample; 8 – stationary sleeve; 9 – sliding axle; 10 – curved lever; 11 – dynamometer; 12 – eccentric wheel.

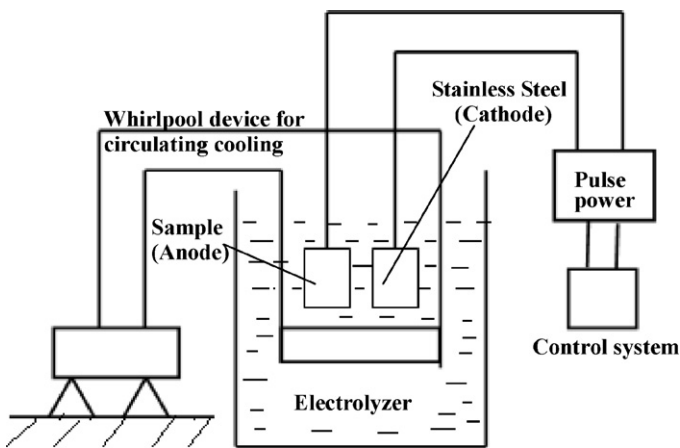


Fig. 2. Schematic drawing of the PEO equipment.

$710 \pm 10^\circ\text{C}$. The pretreatment procedures are sand-paper grinding, alkaline cleaning, picking and alcohol scrubbing prior to the hot-dipping process. The device used for hot-dipping here is a well-type self-made crucible resistance furnace as shown in Fig. 1.

The PEO process to prepare ceramic coatings on the aluminized steel surface was carried out with a built in-house asymmetric AC power supply of 2 kW as shown in Fig. 2. An aqueous electrolyte containing KOH (8 g/l) and Na_2SiO_3 (10 g/l) in distilled water was used as the electrolysis environment. The coatings deposition conditions were preset at 10 min and $1.5\text{ A}/\text{cm}^2$ for the processing time and processing current density, respectively. Throughout the entire PEO experimental process, the electrolyte temperature was maintained

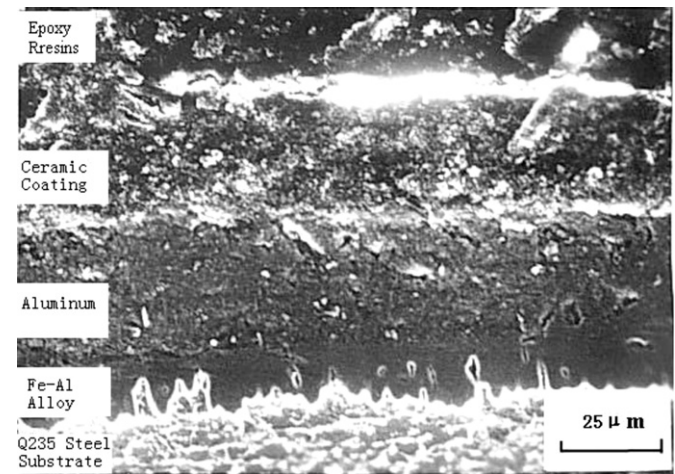


Fig. 4. Cross-sectional SEM morphology of the composite coatings on Q235 steel.

at $40 \pm 2^\circ\text{C}$ constantly using a heat exchanger. After PEO processed, the samples were rinsed thoroughly with water and then were dried in air at room temperature.

The surface morphology and cross-sectional microstructure of HDA-PEO treated samples were examined by a KYKY-2800 scanning electron microscope (SEM). The phase composition of the ceramic coatings was investigated with an H-800 transmission electron microscopy (TEM). The electron acceleration voltage was 200 kV. The TEM samples were prepared by dipping the PEO samples into 3% HCl solution to corrode and remove the Q235 steel and aluminum substrates. Then the pure ceramic flakes were used for TEM observation. D/MAX-rB X-ray diffraction (XRD) with $\text{Cu K}\alpha$ radiation was used to determine the phases present in the

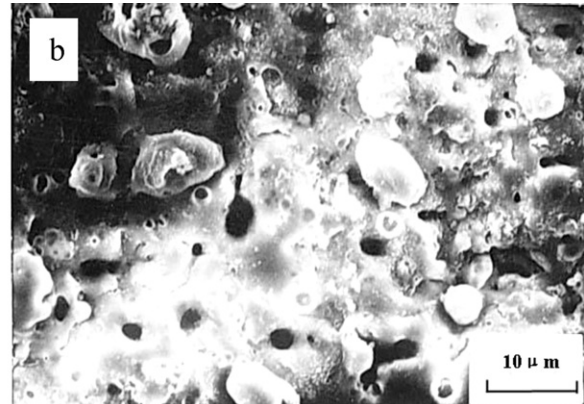
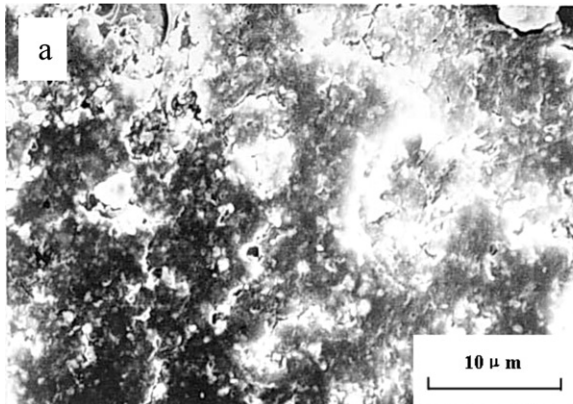


Fig. 5. The cross sectional microstructure (a) and surface SEM morphology (b) of the ceramic coatings.

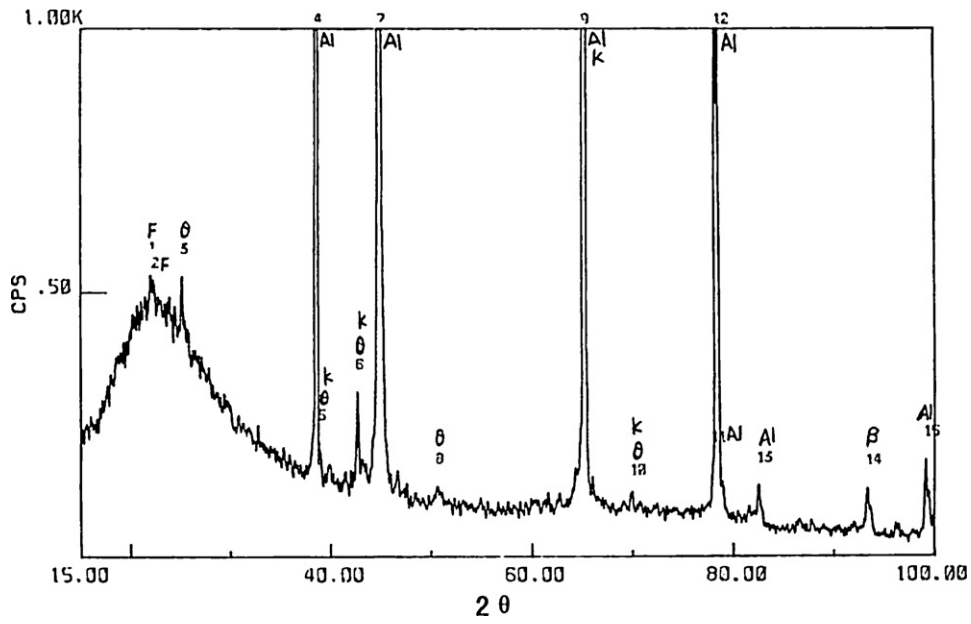


Fig. 6. XRD spectra of the ceramic coatings on Q235 steel. F: amorphous phase; K: κ - Al_2O_3 ; θ : θ - Al_2O_3 ; β : β - Al_2O_3 .

coatings. And scans were performed with 0.01° step size in 2θ range of $15\text{--}100^\circ$. The electron acceleration voltage was 40 kV and the current was 60 mA. The cross-sectional micro-hardness of the treated samples was measured using an AVS-1000 microscopic hardness meter (MHM) at a load of 1.96 N and for a loading duration of 10 s. The wear resistance of the ceramic coatings was investigated by a

self-made rubbing wear testing machine, as shown in Fig. 3. A heat treated 45# steel coupon ($25\text{ mm} \times 10\text{ mm} \times 2.5\text{ mm}$) with 840°C quenching and 150°C tempering was used as the compared body. The weight loss of the PEO and heat treated 45# steel samples was determined by a TG328A electric-light analysis balance (ELAB).



a- Microstructure



b- Diffraction pattern

- $020\theta/302\kappa$
- $113\theta/116\beta$
- $102\theta/002\kappa102\beta$

Fig. 7. TEM information for multi-crystal areas in the PEO ceramic coatings.

3. Results and discussion

3.1. Cross-sectional microstructure and surface morphology of the composite coatings

Fig. 4 shows the scanning electron micrograph of the typical cross-section of the HDA-PEO coated specimen. It can be seen that the specimen is covered with a composite coatings which consists of three layers. They are Fe–Al alloy layer next to the steel substrate, aluminum layer near the Fe–Al alloy layer, and oxide ceramic layer as a top exterior layer. Obvious wavy jagged interface can be observed between all the linked two layers or between the Fe–Al alloy layer and the steel substrate, which is reasonable as a result of the chemical or electro-chemical reaction between each of the two layers described above. So metallurgical bonding has become the interface character among them, including the whole composite layer and the steel substrate.

The cross-sectional microstructure and surface morphology of the ceramic coatings are shown in Fig. 5. As can be seen, the ceramic coatings exhibits a typical PEO porous structure. Fig. 5a shows that there are many micro-cracks in the PEO ceramic coatings. It is assumed that the development of such defects in the PEO coatings is attributed to the thermal stresses during the coatings evolution, which are resulted from melting–solidifying and discharging, and some other fast heating–cooling processes all over the growth process of the ceramic coatings. Fig. 5b shows the fabrication of coatings from numerous, fused and dense-packed particles whose

size varied within 5–10 μm because of the quick re-melting and solidification of the particles in local zones. And it also demonstrates numerous and quite non-uniformly distributed globe-like pores showing the density, size and spacing of discharge channels during the coatings growth. Through the discharge channels the Al and Al^{3+} from the substrate were likely ejected onto the coating/electrolyte interface during the plasma-caused melting, then combined with the O^{2-} generated by OH^- in the electrolyte, and finally sintered and deposited on the coating surface, contributing to the coating growth. With the processing time of PEO prolonged, some of discharge channels were plugged by the particles. These particles would be molten and buried by later oxidation mass, and become parts of the coatings finally. Unlike the cross-sectional morphology, there are no obvious micro-cracks besides micro-pores on the surface morphology images of the PEO ceramic coatings.

3.2. Phase composition of the ceramic coatings

Typical XRD pattern of the composite ceramic coatings on Q235 steel is shown in Fig. 6. The coatings is partly crystallized and mainly composed of amorphous alumina, a proportion of above 80%. The result may come from the quite fast cooling rate of molten alumina. Krysmann considered that the temperature in micro-arc zones could reach 8000 K within 10–15 μs [14]. Therefore, cooling rate could be up to 106 K/s for melting alumina due to the fact that the melting point of alumina is above 2300 K and the temperature of the solution around the specimens is about 300 K. The



a- Microstructure



b- Diffraction pattern

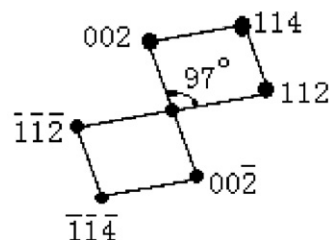


Fig. 8. TEM of $\kappa\text{-Al}_2\text{O}_3$ single crystal areas in the PEO ceramic coatings.

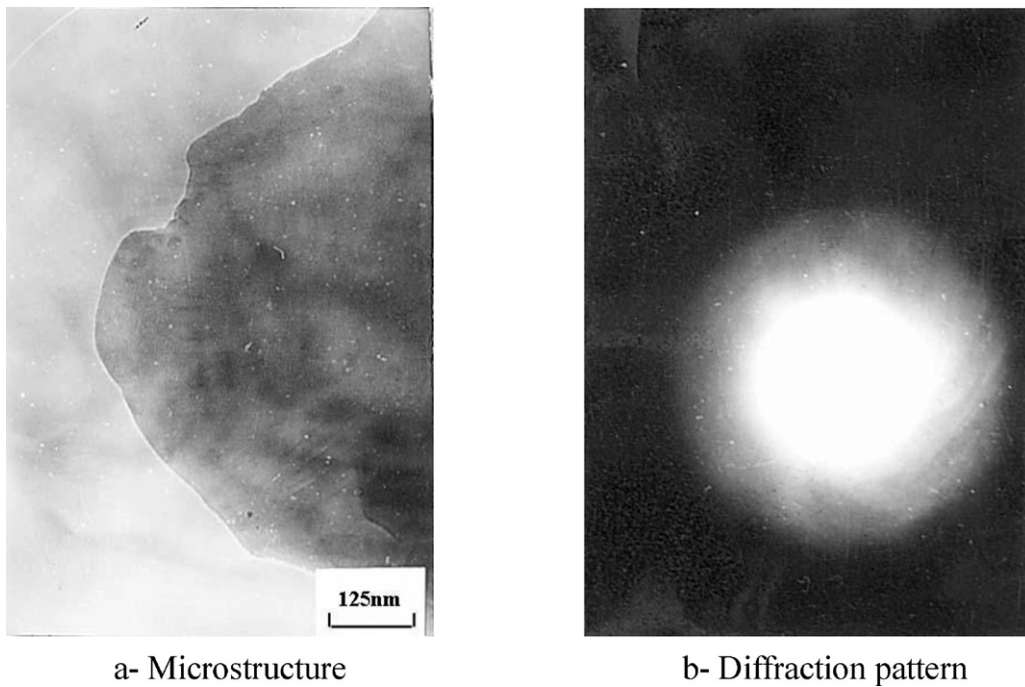


Fig. 9. TEM of the amorphous areas in the PEO ceramic coatings.

Table 1

d-Spacing values from the test results and the ASTM card data.

<i>d</i> -Spacing values from the test (Å)	Some <i>d</i> -spacing values of Al ₂ O ₃ in ASTM card (Å)		
	θ-Al ₂ O ₃	κ-Al ₂ O ₃	β-Al ₂ O ₃
4.326	4.50	4.50	4.45
2.222	2.24	–	2.24
1.468	1.45	1.45	–

rest phase composition of the ceramic coatings is κ-Al₂O₃, θ-Al₂O₃ and β-Al₂O₃. Among them, the content of β-Al₂O₃ is the least. The density of the Al diffraction lines in the typical XRD pattern is far stronger than that of the alumina ceramic phase, which implies that the X-ray diffracted layer is composed of elemental Al from the hot-dipped Al substrate, therefore the ceramic coatings is not very thick, which is about 40 μm measured with micrometer.

TEM results for the compact layer of the ceramic coatings are shown in Fig. 7. As seen in Fig. 7a, the coatings are composed of quite non-uniform crystal particles. The size of some smaller grains is less than 100 nm and some others is over 500 nm or even bigger (Fig. 8a), so that single crystal diffraction pots can be observed from

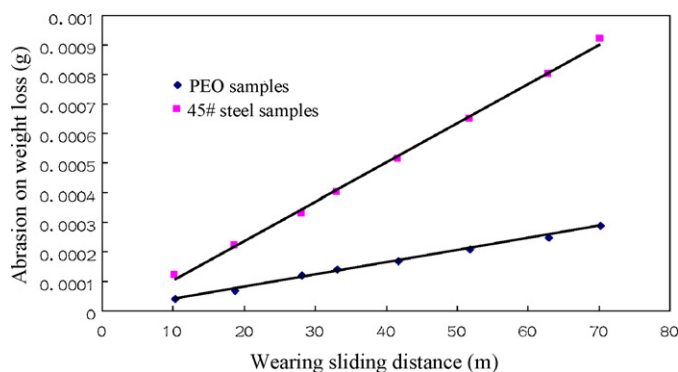


Fig. 10. Abrasion weight-loss curves of the coatings and the heat treated 45# steel.

these areas where bigger grains stand, such as diffraction pots of κ-Al₂O₃ shown in Fig. 8b.

Fig. 7b shows the polycrystalline character and even amorphous rings of the coatings. Both *d*-spacing values from the test results and ASTM card data are listed in Table 1.

Besides amorphous phase, as shown in Table 1, the phase composition of the ceramic coatings also contains θ-Al₂O₃, κ-Al₂O₃ and β-Al₂O₃, which is consistent with the previous XRD results. The TEM bright field photograph and corresponding diffraction pattern of the typical amorphous zone are shown in Fig. 9a and b, respectively.

3.3. Wear resistance and cross-sectional micro-hardness of the composite coatings

The abrasion weight loss was used to measure the wear resistance of the samples. The less the abrasion weight loss is, the better the wear resistance is. The wear resistance of PEO samples and the heat treated 45# steel samples with 840 °C quenching and 150 °C tempering are shown in Fig. 10. It is clear that the wear resistance of the PEO samples is better than that of the heat treated 45# steel

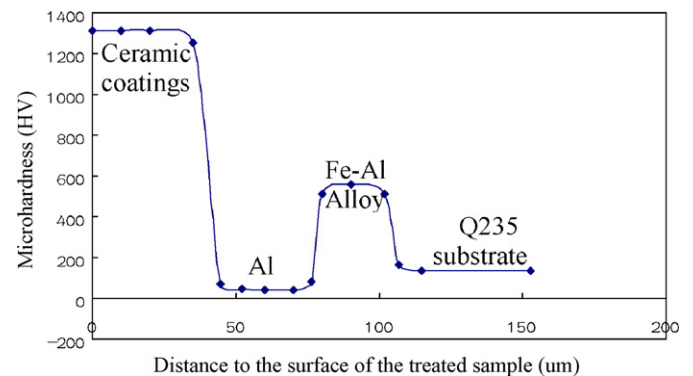


Fig. 11. Hardness distribution along the cross-section of the HDA-PEO coated sample.

samples. When the wearing sliding distance is 70 m, the weight loss of the heat treated 45# steel samples is about 3 times higher than that of the PEO samples, which implies that the wear resistance of the PEO samples is about 3 times higher than that of the heat treated 45# steel.

The high hardness of the coatings was favorable to the better wear resistance. Moreover, the dense structure of the layer (Fig. 5(a)) might considerably improve the load-bearing capacity of the coatings. The cross-section micro-hardness of the HDA-PEO coated sample was shown in Fig. 11. It can be seen that the hardness of the ceramic coatings composed of θ -Al₂O₃, κ -Al₂O₃ and β -Al₂O₃ is about HV1300, which is the highest among the cross-section hardness of the HDA-PEO coated sample, about 10 times higher than that of the Q235 substrate.

4. Conclusions

Hot-dipping aluminum process and plasma electrolytic oxidation process were carried out separately and the composite ceramic coatings on Q235 steel were obtained with the hybrid method.

The conclusions from the characteristics and wear resistance of the composite coatings investigation are as follows:

- (1) There are many micro-pores and cracks in the plasma electrolytic oxidation ceramic coatings, which result in the discharge channels all over the ceramic coatings.
- (2) The phase composition of the ceramic coatings is mainly amorphous phase and crystal Al₂O₃ oxides. The crystal Al₂O₃ oxides include κ -Al₂O₃, θ -Al₂O₃ and β -Al₂O₃. The grain size of the κ -Al₂O₃ crystal is quite non-uniform. The smallest ones was less than 100 nm and the biggest ones was more than 500 nm or even larger. So that the single crystal diffraction pattern of the κ -Al₂O₃ can be obtained.
- (3) The hardness of the ceramic coatings is about HV1300 and 10 times higher than that of the Q235 substrate, which was favorable to the better wear resistance of the ceramic coatings. When

the wearing sliding distance is up to 70 m, the wear resistance of the PEO samples is about 3 times higher than that of the heat treated 45# steel.

Acknowledgements

The research is funded by Hebei Province Natural Science Foundation under Grant No. A2011203068, especially the project "Control method and mechanism on breakdown resistance equilibrium of ceramic coatings by micro-defect induction during PEO process" supported by National Natural Science Foundation of China under Grant No. 51171167.

References

- [1] K. Wang, J.K. Young, H. Yasunori, G.L. Chan, H.K. Bon, *Journal of Ceramic Processing Research* 10 (2009) 562–566.
- [2] S. Stojadinovic, R. Vasilic, I. Belca, M. Petkovic, B. Kasalica, Z. Nedic, Lj. Zekovic, *Corrosion Science* 52 (2010) 3258–3265.
- [3] Y. Yang, H. Wu, *Transactions of Nonferrous Metals Society of China* 20 (2010) s688–s692.
- [4] A.L. Yerokhin, A. Shatrov, V. Samsonov, P. Shashkov, A. Pilkington, A. Leyland, A. Matthews, *Surface and Coatings Technology* 199 (2005) 150–157.
- [5] W. Xue, C. Wang, R. Chen, Z. Deng, *Materials Letters* 52 (2002) 435–441.
- [6] R. Arrabal, E. Matykina, F. Viejo, P. Skeldon, G.E. Thompson, *Corrosion Science* 50 (2008) 1744–1752.
- [7] X. Lin, M. Zhu, J.-F. Zheng, J. Luo, J. Mo, *Transactions of Nonferrous Metals Society of China* 20 (2010) 537–546.
- [8] B. Kasalica, M. Petkovic, I. Belca, S. Stojadinovic, Lj. Zekovic, *Surface and Coatings Technology* 203 (2009) 3000–3004.
- [9] D. Shen, Y. Wang, W. Gu, G. Xing, *Transactions of Nonferrous Metals Society of China* 14 (2004) 170–173.
- [10] Z. Wu, Y. Xia, G. Li, F. Xu, *Acta Metallurgica Sinica* 44 (2008) 119–124.
- [11] W.C. Gu, D.J. Shen, Y.L. Wang, G.L. Chen, W.R. Feng, G.L. Zhang, S.H. Fan, C.Z. Liu, S.Z. Yang, *Applied Surface Science* 252 (2006) 2927–2932.
- [12] V. Pokhmurskii, H. Nykyforchyn, M. Student, M. Klapkiv, H. Pokhmurska, B. Wielage, T. Grund, A. Wank, *Journal of Thermal Spray Technology* 16 (2007) 998–1004.
- [13] P. Zhang, X. Nie, H. Hu, Y. Liu, *Surface & Coatings Technology* 205 (2010) 1508–1514.
- [14] W. Krysmann, P. Kurze, K.H. Dittich, *Crystal Research and Technology* 19 (1984) 973–979.